**RESEARCH ARTICLE**

# Application of Mixture of Experts in Machine Learning-Based Controlling of DC-DC Power Electronics Converter

**MOHSEN MOHAMMADZADEH[1], EHSAN AKBARI[2], ANAS A. SALAMEH[3],**
**MOJTABA GHADAMYARI[4], (Member, IEEE), SASAN PIROUZI[5],**
**AND TOMONOBU SENJYU[6], (Senior Member, IEEE)**

[1]Faculty of Electrical and Computer Engineering, Noshirvani University of Technology, Babol 47148-71167, Iran
[2]Department of Electrical Engineering, Mazandaran University of Science and Technology, Babol 47166-85635, Iran
[3]Department of Management Information Systems, College of Business Administration, Prince Sattam Bin Abdulaziz University, Al-Kharj 11942, Saudi Arabia
[4]Department of Computer Engineering, Lebanese French University, Kurdistan Region 44001, Iraq
[5]Power System Group, Semirom Branch, Islamic Azad University, Semirom 8514143131, Iran
[6]Faculty of Engineering, University of the Ryukyus, Okinawa 903-0213, Japan

Corresponding authors: Tomonobu Senjyu (b985542@tec.u-ryukyu.ac.jp) and Sasan Pirouzi (s.pirouzi@sutech.ac.ir)

**ABSTRACT** Regardless of the application in which power electronic converters are deployed, their desired performances crucially depend on the controlling strategy while different impressive parameters are varied. This paper offers a novel controlling strategy originated from the mixture of two well-known controlling techniques, namely feedback (FBC) and model predictive (MPC) controllers. It uses the advantages of the above-mentioned controllers while their drawbacks or limitations are covered by each other using the mixture of experts (MoE) technique. Two neural networks for capturing the features of MPC and FBC along with a gating network as the main tool of MoE are employed in order to optimize the controlling of the DC-DC power electronic converters. These networks are trained through a set of pair data as the input vector and the target data. The results reveal that better performance can be obtained via benefit exploitation of both controlling techniques using a comprehensive MoE. The dynamic and steady state errors are decreased by 5% and 8%, respectively which demonstrate a global enhancement in the controlling of the DC-DC power electronic converters.

**INDEX TERMS** Mixture of experts, machine learning, power electronic converters (PECs), controlling strategy.

## NOMENCLATURE

| | |
|---|---|
| $C$ | Output capacitor. |
| $d$ | Duty cycle. |
| $e$ | Error between actual and reference variable. |
| $f_s$ | Switching Frequency. |
| $i_L$ | Current of input inductor. |
| $I_{Lref}$ | Reference inductor current. |
| $I_L^{SS}$ | Steady state inductor current. |
| $I_{s0}$ | Initial value of inductor current. |
| $L$ | Input inductance. |
| $Q$ | Power switch. |
| $q$ | Gate signal. |
| $R_C$ | Internal resistance of output capacitor. |
| $R_L$ | Internal resistance of input inductor. |
| $R_o$ | Load resistance. |
| $T_s$ | Switching. |
| $u(t)$ | Switching function. |
| $v_C$ | Voltage of output capacitor. |
| $V_{Cref}$ | Reference capacitor voltage. |
| $V_C^{SS}$ | Steady state capacitor voltage. |
| $V_{in}$ | Input Voltage. |
| $v_L$ | Voltage of input inductor. |

## I. INTRODUCTION

Modern advances in materials and manufacturing process of power electronics have pushed back the frontiers of their applications every day [1], [2], [3], [4]. The harnessing of these technologies in all sorts of creative ways plays a crucial role in designing and controlling the power electronic converters. Controlling techniques are in charge of meeting several principle requirements including static operation, dynamic operation, fault management & protection, and reliability-related aspects [5], [6], [7], [8], [9]. Recently, a significant number of studies have paid attention to the controlling techniques of the power electronics converters [10], [11], [12]. Conventional output feedback (voltage mode or current mode) has been widely used owing to its simple implementation. The conventional linear output feedback controllers have been enhanced using complementary techniques such as flux-based techniques [13], [14], charge-based techniques [15], [16], and geometry control [17]. Although these structures are identical to the voltage mode controller, their performances are much more robust and less noisy (more identical to the current mode controller).

Another widely used control method is ripple-based techniques which are originated from hysteresis controls [18]. Switching frequency is variable and the controller may be unstable in the cases in which the equivalent series resistor (ESR) of the output capacitor is significant [19]. Zhou et al. [12] proposed an enhanced ripple-based control in which ESR voltage ripple is estimated and considered in the control loop. However, the method is suitable for large ESR power capacitors which is not the case in real applications. Because the higher the ESR is, the more sub-harmonics (and consequently the larger voltage ripple) are generated.

Since electronic chips have become cost-effective, employing digital-based controlling techniques has attracted attention among researchers [20], [21], [22]. A high bandwidth inductor current estimator for digitally controlled dc-dc converters is proposed in [23]. The proposed technique tries to estimate the inductor current with the capability of considering independent gains for average and ripple components. This inductor current estimator is employed in a digital current hysteresis control. Zhou et al. [24] proposed a digital average voltage/digital average capacitor current with a dual-edge modulation technique. Although the method demonstrates a fast transient performance, it requires a digital compensator for increasing output regulation accuracy which leads to a larger memory size of microprocessors in comparison with the digital average-ripple-based control techniques.

The observer-based control technique can be considered as an alternative for the state variable feedback controller [25]. Peltoniemi et al. [26] have used an integrator tracker for inductor voltage to guarantee that the inductor voltage is averagely zero during one cycle. These kinds of controllers are related to the model reference adaptive controller [7], [27]. The combination of the observer-based and model reference adaptive control techniques has launched a control category

of model predictive controls (MPC) [28]. Recently, several researchers have undertaken different MPC techniques in the various converters [29], [30], [31], [32]. As an example in [32], a finite control set MPC (FCS-MPC) has been proposed based on a logical dynamic model. An inner current loop controller, as well as an outer voltage loop controller, are used in the proposed structure. Variable switching frequency and lack of generating an accurate current reference are the constraints of this method which the latter may be alleviated by the technique presented in [33]. The variable switching frequency of the aforementioned method has been tackled with the proposed formulated approach in [34] called continuous control set MPC (CCS-MPC). Enhancement of reference current generation along with the fixed switching frequency make CCS-MPC an attractive approach in DC-DC converters controlling.

Another solution for improving control performance of DC-DC power converter is described in [35]. In this work, an adaptive deep learning-based technique has been proposed in order to mitigate some uncontrolled steady-state voltage deviations. In the wide range of switching frequencies, the proposed method prepares a precise voltage gain using particle swarm optimization for discovering the optimal operating point which rapidly adjusts voltage gain and suppresses the steady-state voltage deviation. However, the transient behavior of the converter has not been considered and the converter is not well controlled in the severe load and input disturbances. Deep reinforcement learning based controlling technique has been recently employed in several applications [36], [37], [38]. These researches apply the reinforcement learning on the different strategies such as sliding mode and model predictive for enhancing the transient and steady state behavior of the DC-DC converters. These approaches suffer from huge off-line computations and large size of memory for online processing and optimizing the performance of the converter. In addition, several optimization algorithms including Bat algorithm [39], Bee algorithm [40], and genetic algorithm [41], [42] have been proposed in order to optimize the parameters of conventional controller. Although these algorithms explore to optimize the controlling parameters of a specific controller for improving the response of the converter, their optimizations are limited to some confined controlling indices. Thus, they are still lacking a global optimization for extended numbers of controlling indices including setting time, over/undershoot, steady state voltage ripple, power loss, etc.

Even though the performance of the power electronic DC-DC converters has been improved in recent years by employing aforementioned controlling strategies, most improvements have been achieved by optimizing some key indices at the expense of deteriorating the other indices. Nonetheless, it is possible to further improve this performance by possessing the advantages of more than one controlling strategies through mixture of experts (MoE) and artificial intelligence (AI) approaches. In this study, output feedback control (FBC) and model predictive

controller (MPC) are considered as two experts for optimizing different aspects of the controlling system. FBC has been widely used due to its simple design and implementation. Furthermore, the FBC technique better manages steady-state, power loss, output voltage ripple, and robustness against parameter deviation. However, MPC is well known for its dynamic response performance. The MPC introduces a better settling time and voltage overshoot/undershoot. With this goal, this work seeks to simultaneously

1- improve the steady state indices of the converter such as power loss, output voltage ripple, and robustness against parameter deviation by increasing the FBC contribution and

2- improve the transient indices of the converter such as settling time and voltage overshoot/undershoot by increasing the MPC contribution in the global controlling system.

In this regard, MPC and FBC techniques are separately implemented using two distinct neural networks. The neural networks are trained using a real mission profile by considering the inductor current and capacitor voltage as the input data and switching state as the target. The share of each technique in controlling the power converter is allocated with MoE.

The remainder of this paper is structured as follows. Section II presents the DC-DC boost power electronics converter modeling and introduces the FBC and MPC techniques. Section III presents a case study and investigates the related mission profile and the neural network training algorithm. Section IV deals with MoE definitions and formulations. Section V expresses the numerical results, experimental results, and additional discussions. The concluding remarks are eventually drawn in Section VI.

## II. CONVENTIONAL DC-DC BOOST POWER ELECTRONICS CONVERTER

In this study, we propose a combined controlling strategy for a DC-DC power converter employing two well-known controlling techniques, namely FBC and MPC. As shown in Fig. 1, two neural networks are trained by FBC and MPC controllers in such way to estimate the controlling variable (switching function $u(t)$) by knowing the states of the input inductor current and the output capacitor voltage. Another unit called mixture of experts defines the contribution of each controlling strategy in the controlling variable via the input states, namely input inductor current and output capacitor voltage and using a gating network. The resulted controlling variable ($u(t)$) is, then, inserted to the pulse width modulation (PWM) unit for generating the gate signals for the main switches of the converter.

Conventional DC-DC boost power electronics converter (DC-DC BPEC) has been widely used in diverse applications such as renewable energy, energy storage, and automotive systems [42], [43], [45]. Fig. 2 illustrates the circuit topology of the DC-DC BPEC. The circuit consists of several passive components and an active MOSFET switch. $L$ and $C$ are the inductor and the output capacitor which their equivalent series resistances are represented by $R_L$ and $R_C$, respectively. $Q$ and $D$ are the power switch and diode, respectively. Output
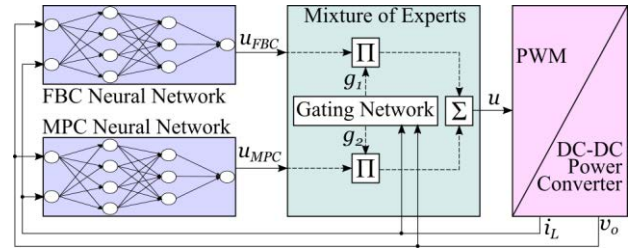


**FIGURE 1.** Block diagram of the proposed controlling strategy based on mixture of experts, namely FBC and MPC.

voltage and inductor current are sensed and processed in the controllers (FBC or MPC) and the controllers provide a switching signal which is transformed to the gate signal using a modulation technique and a gate driver.

### A. DC-DC BOOST POWER ELECTRONICS CONVERTER MODEL

The continuous model of DC-DC BPEC can be written as follows in both continuous conduction mode (CCM) and discontinuous conduction mode (DCM) using a binary function of $d_{aux}$ [34], [46]

$$
\begin{aligned}
\frac{di_L(t)}{dt} &= \frac{R_o}{L(R_o+R_C)}(R_C i_L(t)+v_C(t))u(t) \\
&+ d_{aux}\left(\frac{-R_L}{L}-\frac{R_o R_C}{L(R_o+R_C)}\right)i_L(t) \\
&- d_{aux}\frac{R_o}{L(R_o+R_C)}v_C(t)+d_{aux}\frac{v_{in}(t)}{L} \\
\frac{dv_C(t)}{dt} &= d_{aux}\frac{R_o}{C(R_o+R_C)}i_L(t)-\frac{1}{C(R_o+R_C)}v_C(t) \\
&- \frac{R_o}{C(R_o+R_C)}i_L(t)u(t) \\
v_o(t) &= d_{aux}\frac{R_o R_C}{(R_o+R_C)}i_L(t)+\frac{R_o}{R_o+R_C}v_C(t) \\
&- \frac{R_o R_C}{(R_o+R_C)}i_L(t)u(t)
\end{aligned} \tag{1}
$$

where $u(t)$ is the switching state (system input) and $d_{aux}(t)$ represents the operating mode of DC-DC BPEC in which *1* means CCM while *0* means DCM operation.

$$
u(t) = \begin{cases} 1 & q=1 \\ 0 & q=0 \end{cases}
$$

$$
d_{aux}(t) = \begin{cases} 1 & u(t)\geq 0 \ and \ i_L(t)>0 \\ 0 & u(t)=0 \ and \ i_L(t)=0 \end{cases} \tag{2}
$$

From the continuous-time model described in eq. (1), one can obtain the discrete-time model ignoring the higher-order terms as follows:

$$
\begin{aligned}
x(k+1) &= Ax(k)+Bu(k)+Ev \\
y(k) &= Cx(k)+Du(k) \\
u(k) &= \begin{cases} 1 & q=1 \\ 0 & q=0 \end{cases}
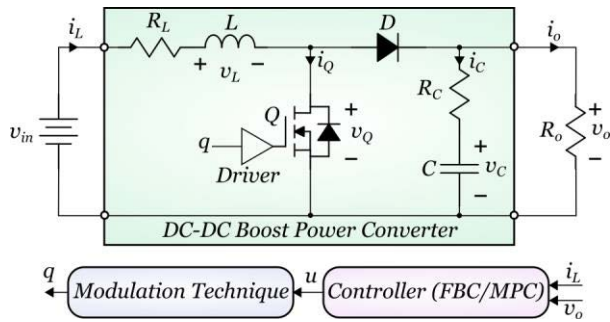\end{aligned} \tag{3}
$$

**FIGURE 2.** Circuit topology of the DC-DC boost power converter. Inductor current and output voltage are sensed for FBC and MPC controllers. The controllers provide a switching signal which may drive the main switch using a modulation technique and a driver.

where $x$, $y$, and $u$ are the state, output, and input vectors, respectively. $A$, $B$, $C$, $D$, and $E$ are the constant-coefficient matrices and are written as follows

$$x(k) = [i_L(k)v_C(k)]^T$$
$$y(k) = [i_L(k)v_O(k)]^T$$

$$A = \begin{bmatrix} 1 - \tau_{aux}[\dfrac{T_s R_L}{L} + \dfrac{T_s R_O R_C}{L(R_O + R_C)}] & \tau_{aux}\dfrac{-T_s R_O}{L(R_O + R_C)} \\ \tau_{aux}\dfrac{T_s R_O}{C(R_O + R_C)} & 1 - \dfrac{T_s}{C(R_O + R_C)} \end{bmatrix}$$

$$B = \begin{bmatrix} \dfrac{T_s R_O}{L(R_O + R_C)}(R_C i_L(k) + v_C(k)) \\ -\dfrac{T_s R_O}{C(R_O + R_C)} i_L(k) \end{bmatrix}$$

$$C = \begin{bmatrix} 1 & 0 \\ \tau_{aux}\dfrac{T_s R_O}{R_O + R_C} & \dfrac{R_O}{(R_O + R_C)} \end{bmatrix}$$

$$D = \begin{bmatrix} 0 \\ \dfrac{-T_s R_O}{R_O + R_C} i_L(k) \end{bmatrix}, \quad E = \begin{bmatrix} \tau_{aux}\dfrac{T_s}{L} \end{bmatrix}, \quad v = v_{in}(k)$$

$$(4)$$

$\tau_{aux}$ is an auxiliary variable for representing the diverse operating conditions of the DC-DC BPEC in which the inductor current experiences different manners in a single switching period [34] and written as follows:

$$\tau_{aux} = \begin{cases} 1 & u(k) \geq 0 \text{ and } i_L(k+1) > 0 \\ \dfrac{t_1}{T_s} & u(k) = 0 \text{ and } i_L(k+1) = 0 \text{ and } i(k) > 0 \quad (5) \\ 0 & u(k) = 0 \text{ and } i_L(k) = 0 \end{cases}$$

where $t_1$ represents the taken time duration in which the inductor current reaches zero just after the switching period begins.

## B. FEEDBACK CONTROLLER

The feedback controller is a well-known extensively used controlling strategy in real applications due to its easy implementation and undeniable properties including low voltage

ripple, low steady-state error, low power loss, and more robust against parameters deviation of DC-DC BPEC converter. Stability analysis of the zero dynamics (internal dynamics) and the minimum phase property of the inductor current served as the output state hand-in-hand can be employed for indirect controlling of the capacitor voltage (output voltage) while it is not the case in which the capacitor voltage is served as the direct output of state [47], [48]. Regarding equation (1) and considering that capacitor voltage and inductor current are unchanged in a switching period, the following equation can describe the relation between capacitor voltage and inductor current.

$$V_C^2 + R_C I_L V_C = d_{aux}[(R_o R_C + (R_o + R_C) v_{in}) I_L \\ - (R_o R_C + (R_o + R_C) R_L) I_L^2] \quad (6)$$

If consider that the second term in the left side of the equation (6) is much smaller than the first term which is the case while the capacitor equivalent series resistance is ignorable and the DC-DC BPEC is in CCM operating mode ($d_{aux} = 1$), one can rewrite equation (6) as follows:

$$V_{Cref} = \sqrt{\begin{array}{c}(R_o R_C + (R_o + R_C) v_{in}) I_{Lref} \\ - (R_o R_C + (R_o + R_C) R_L) I_{Lref}^2\end{array}} \quad (7)$$

where $V_{Cref}$ and $I_{Lref}$ are the reference value of the capacitor voltage and inductor current, respectively. With regard to equation (7), one can find that the capacitor voltage can be adjusted around the desired value through the appropriate associated adjustment of the inductor current while output load and input voltage are unchanged. Let define a new variable for the output derivative ($\varphi = \dot{y} = di_L(t)/dt$), the controlling signal ($u(t)$) can be derived as follows using the extracted equation (1)

$$\varphi = \frac{R_o}{L(R_o + R_C)}(R_C i_L(t) + v_C(t)) u(t) + \frac{v_{in}(t)}{L} \\ - \frac{R_o}{L(R_o + R_C)} v_C(t) + \left(\frac{-R_L}{L} - \frac{R_o R_C}{L(R_o + R_C)}\right) i_L(t) \quad (8)$$

The controlling signal is calculated as

$$u(t) = \frac{1}{(R_C i_L(t) + v_C(t))}(\frac{(R_o + R_C)}{R_o}\varphi L + v_C(t) \\ + \left(\frac{(R_o + R_C) R_L}{R_o} + R_C\right) i_L(t) - \frac{(R_o + R_C)}{R_o} v_{in}(t)) \quad (9)$$

Assume that the inductor current tracks the error of $e = I_{Lref} - i_L(t)$, then

$$\varphi = \dot{y}_{ref} + ke = k(I_{Lref} - i_L(t)) \quad (10)$$

where k is a positive coefficient that can be chosen by suitable pole assignment to ensure inductor current error converges to zero asymptotically. Inserting equation (10) into equation (9)

$$u(t) = \frac{1}{(R_C i_L(t) + v_C(t))}(\frac{(R_o + R_C) k(I_{Lref} - i_L(t))}{R_o} L$$
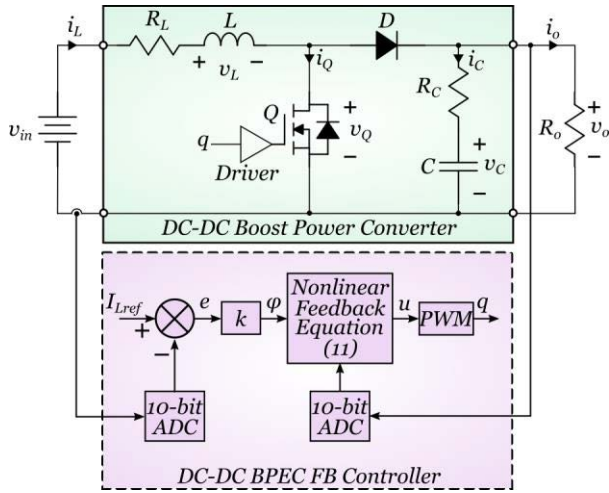
**FIGURE 3.** Controlling the DC-DC BPEC converter using a two-closed-loop feedback controller via providing a switching signal for driving the main switch. Inductor current and capacitor voltage are sensed, converted to the 10-bit digital signal, and applied to the controlling algorithm.

$$+ \left( \frac{(R_o + R_C) R_L}{R_o} + R_C \right) i_L(t)$$
$$+ v_C(t) - \frac{(R_o + R_C)}{R_o} V_{in}) \tag{11}$$

Accordingly, a two-closed loop can be designed and applied to the DC-DC BPEC for the control of the output voltage as shown in Fig. 3.

### C. MODEL PREDICTIVE CONTROLLER

The model predictive controller has been introduced since the programmable microcontroller or digital signal processors had widely used in electronic systems. The results of using MPC reveal a better dynamic performance of DC-DC power electronic converters. Although several studies have proposed diverse model predictive controlling algorithms including finite control set MPC (FCS-MPC) [29] and continuous control set MPC (CCS-MPC) [20], the proposed MPC controller in [34] with the reduced prediction horizon and the fixed switching frequency is used here.

Capacitor voltage and inductor current both may consider to be constant during a period of switching regarding equation (1) and the assumption that the natural frequencies of the BPEC DC-DC converter are much higher than switching frequency. Therefore, following equation can describe inductor current increment regarding Fig. 4.

$$i_L(k + 1) = i_{s0} + f_{L1}t_1 + f_{L2}t_2 + f_{L3}t_3 \tag{12}$$

where

$$f_{L1} = \frac{V_{in}}{L}, \quad f_{L2} = \frac{V_{in} - V_C(k)}{L}, \quad f_{L3} = \frac{V_{in}}{L} \tag{13}$$

And $i_{s0}$ is the initial value of $i_L(k)$. A standard current tracking error may be written as
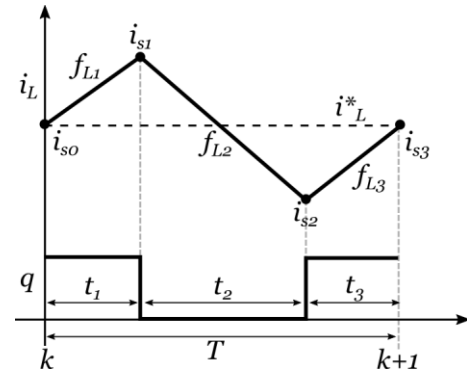
$$J(k) = (i_L(k + 1) - i_L^*(k + 1))^2$$



**FIGURE 4.** Inductor current during one single switching period.

$$= (e_L - f_{L1}t_1)^2 + (e_L - f_{L1}t_1 - f_{L2}(T - 2t_1))^2$$
$$+ (e_L - f_{L1}t_1 - f_{L2}(T - 2t_1) - f_{L3}t_1)^2 \tag{14}$$

where $e_L = i_L^*(k + 1) - i_L(k)$ is the inductor current tracking error. If $t_1$ and $t_3$ are equal and accordingly $i_{s0}$ and $i_{s3}$ equal to the average value of the inductor current ($i_L(k)$) as shown in Fig. 4. With differentiating $J(k)$ in term of $t_1$ and equaling it to zero ($dJ(k)/dt_1 = 0$), the optimized timing can be found as

$$t_1 = \frac{4e_L - 3Tf_{L2}}{6(f_{L1} - f_{L2})} \quad t_2 = T - 2t_1 \ t_3 = t_1 \tag{15}$$

The steady-state (SS) reference inductor current and capacitor voltage may be defined as follows based on equation (1)

$$V_C^*(k + 1) = V_C^{SS}$$

$$i_L^*(k + 1) = \frac{V_{in}}{2R_L} - \sqrt{\left( \frac{V_{in}}{2R_L} \right)^2 - \frac{(V_C^{SS})^2}{R R_L}} \tag{16}$$

Since there exist uncertainties in the load, a standard Lungberger observer is used to compensate the model in facing uncertainties [28], [34]. Fig. 5 demonstrates the global structure of CCS-MPC controlling system. The details of the controlling system can be found in [34]. As shown, Capacitor voltage is sensed for standard Lungberger observer in order to compensate the load variation during the BPEC DC-DC operating time. Inductor current is also sensed and inserted in to CCS-MPC current controller in order to better estimate the switching time.

## III. MACHINE LEARNING FOR CONTROLLING DC-DC POWER ELECTRONICS BOOST CONVERTER

Machine learning algorithm has been widely used in power electronics [49], [50], [51] along with several other domains [9], [52]. In the different applications, it works as the universal mapping function for capturing the desired target through the best structure of the input data. In this study, a machine learning based controlling strategy has been used in order to optimize the performance of DC-DC BPEC employing the FBC and CCS-MPC structures. Machine learning can use non-parameter models for training itself to create a mapping function for capturing the input-output relationship. This
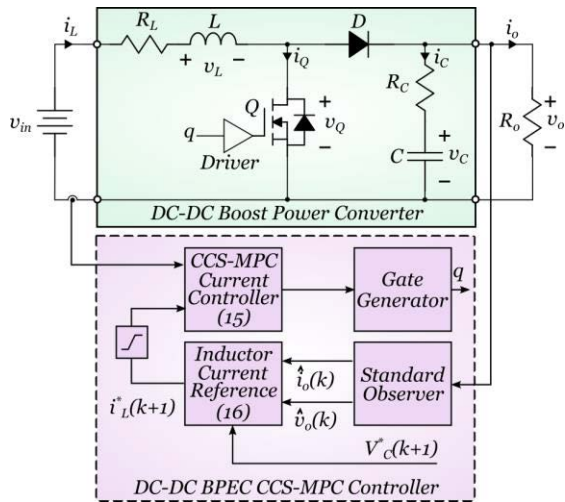
**FIGURE 5.** Controlling the DC-DC BPEC converter using a continuous control set model predictive controller (CCS-MPC) via providing a switching signal for driving the main switch. Inductor current and capacitor voltage are sensed and applied to the controlling algorithm for CCS-MPC compensation and standard Lungberger observation for compensating the load uncertainties.

training is offline and is based on the real world conditions. Fig. 6 demonstrates the machine learning based controlling technique for DC-DC BPEC. As shown, two parameters, namely capacitor voltage and inductor current, are sensed and inserted into the neural network as the input dataset. The output data (target) is the switching function of $u(t)$ which then inserted into the PWM for gate signal generating for the main switch. The trained neural network is a universal function to map the capacitor voltage and the inductor current into a proper gate signal. We define two separate ANNs for controlling the DC-DC BPEC which each of them was trained based on the FBC or MPC techniques. The artificial neural network (ANN) process is described in the following sub-sections.

### A. DATA COLLECTION

For training the neural network an adequate set of input and target data is required. In this study, $v_O$ and $i_L$ are the input data and $u$ is the target or output data. The performance of the ANN will be increased provided that adequate amount of data is collected for training. In this regard, it is assumed that the DC-DC BPEC is working as an interface converter for charging and discharging the battery of an electric vehicle as described in [46]. Thus a mission profile of worldwide harmonized light-duty vehicles driving cycles (WLTC-class3) was considered in this study. WLTC-class3 pattern has 1800 different vehicle speed points for 30min of driving. Regarding the vehicle's specifications, speed and acceleration, the required power can be calculated. Based on the calculated electrical power, the operation points for each of speed point is derived using the DC-DC BPEC model in section II.A. In order to obtain the switching function ($u(t)$) for each operating point, the output capacitor voltage and
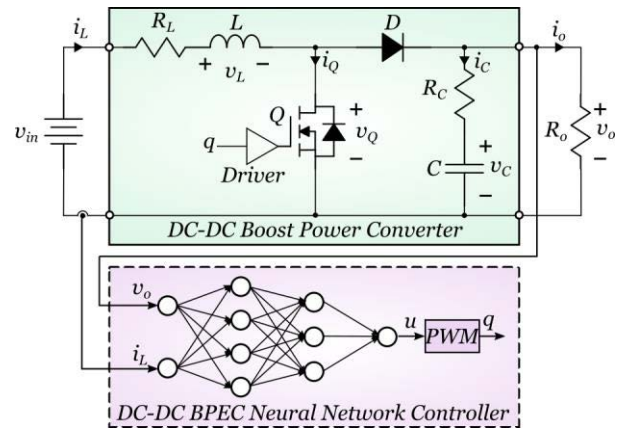


**FIGURE 6.** Controlling the DC-DC BPEC converter using a trained neural network via providing a switching signal for driving the main switch. Inductor current and capacitor voltage are sensed and applied to the controlling algorithm.

input inductor current of the associated operating points are applied to both FBC and CCS-MPC controllers as described in section II.B and section II.C, respectively. The behavior of the DC-DC BPEC ($v_O$ and $i_L$ as the input data and $u$ as the target) was captured for both controlling strategies, namely feedback and model predictive controllers. Accordingly, two distinctive datasets of $[v_O\ i_L u]_{1*3*1800}$ were prepared for each of the controlling strategies and used to train the ANN$_{FBC}$ and ANN$_{MPC}$.

### B. DATA PREPARATION

The contributory candidates ($v_O$ and $i_L$) are considered as the input data for ANN$_{FPCorMPC}$ model ($f_{FBCorMPC}$) to accurately predict the target/desired output (u), i.e. $u = f_{FBCorMPC}(v_O, i_L)$. Thus, a sufficient amount of data may guarantee the accuracy of predictive model namely $f_{FBCorMPC}$. Despite the data may have an extended range of values, it would be better and reported to insert the data into the ANN training process after data rescaling. The input data, namely output capacitor voltage and input inductor current, have different number scales. The value range of these input data are thoroughly different from the output (u) lying between 0 and 1. Accordingly, obtaining the weight coefficients of the neural network for relating these different ranges of values (input versus output) may lead either weak-mapping or diverging. Thus, there is a need to rescale the input data in a range similar to output data (u). In this regard, a range normalization of the data might provide through the following equation:

$$x_{new} = a + \frac{(b-a)(x - min(x))}{max(x) - min(x)} \quad (17)$$

where $x$ and $x_{new}$ are the original and the rescaled data, respectively. $[a, b]$ is the predefined range for data pre-normalization. The best performance under defined conditions were achieved while $a = 0.1$ and $b = 0.9$.

## C. NEURAL NETWORK

There exist several types of neural network for constituting a universal mapping function including artificial neural networks (ANN), convolution neural networks (CNN), recurrent neural networks (RNN) [53], [54]. However, artificial neural network has been used in this study due to simple structure and maturity. The rescaled data as a vector was inserted into the ANN training process. The ANN for both controlling strategies had three hidden layers with the neuron number of 40, 35, and 25, respectively. The input layer has two neurons for receiving $v_O$ and $i_L$ and the output layer has one neuron for indicating the value of the switching function ($u$). The number of hidden layers and their associated neuron numbers were extracted with trials and errors as a trade-off between the training time consumption and the accuracy of the predictions. The layers in the neural network are in charge of information processing in such a way that a precise target (output) is estimated. Each neuron receives the data from the previous neurons with a defined weight and then sum them up with a defined bias and suggest an output for the next layer. In fact, ANN training process tries to obtain the proper values of the weights and the biases of each neuron to reach a desired target with the minimum error. Function of each layer may formulated as follows:

$$\gamma_i^\ell = f \left( \sum_{j=1}^{N_{\ell-1}} \omega_{ij}^l \, \gamma_i^{\ell-1} + b_i \right) \qquad i = 1, \ldots, N_\ell \qquad (18)$$

where $\gamma_i^l$ is the output of the $l^{th}$ and $i^{th}$ layer and neuron, respectively. $\omega_{ij}^l$ and $b_i$ are the weight and biases factors, respectively. $N_l$ and $N_{l-1}$ represent the number of the neuron in $l^{th}$ and $(l-1)^{th}$, respectively. Additionally, $f$ is the Sigmoid activation function. During the training process, the values of $\omega_{ij}^l$ and $b_i$ are obtained in such a way that the minimum root mean square (*RMSE*) and the maximum determination factor ($r$) occurs between the target dataset and the predicted dataset. The *RMSE* and $r$ are defined as follows:

$$RMSE = \sqrt{\sum_{i=1}^{n} \frac{1}{n} \left( \hat{y}_i - y_i \right)^2}$$

$$r = \sqrt{\sum_{i=1}^{n} \left( \hat{y}_i - \bar{y} \right)^2 \bigg/ \sum_{i=1}^{n} \left( y_i - \bar{y} \right)^2} \qquad (19)$$

where $\hat{y}_i$, $y_i$ and $\bar{y}$ are predicted, actual, and the mean value of the actual output, respectively. RMSE values for FBC neural network (ANN$_{FBC}$) and MPC neural network (ANN$_{MPC}$) are calculated as 1.1% and 1.2%, respectively. Accordingly, the trained neural networks with the above-mentioned structures show precise and acceptable mapping functions for relating the inputs to the output.

## IV. MIXTURE OF EXPERTS

Two diverse controlling strategies, namely FBC and MPC, and their features and properties have been discussed in the previous sections. Both of the strategies have their own pros and cons in the controlling DC-DC converters. For integrating
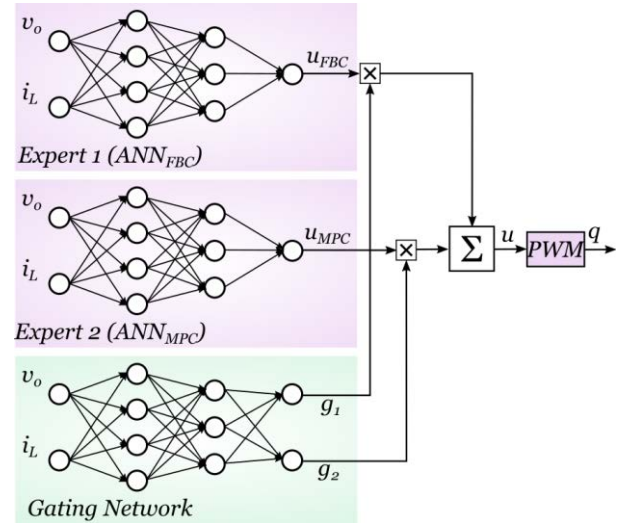


**FIGURE 7.** Architecture of a mixture of experts (MoE) consisting of two expert networks and a gating network. Given an input $x \sim (v_o, i_L)$, the output $y \sim u$ of the system is computed as the sum $u \sim y = \sum_{j=1,2} g_j(x) u_j(x)$.

the benefits and alleviating the drawbacks of these strategies, concept of mixture of experts (MoE) might be used in the controlling of the DC-DC boost power converter. In the proposed MoE controlling strategy as shown in Fig. 7, both of the MPC and FBC are integrated in controlling of the DC-DC BPEC using a gate network which defines the share of each controlling system contribution in determining the target i.e. switching function $u(t)$. The gating network (GN) is a kind of neural network with several hidden layers connecting the inputs to the outputs. The number of the GN inputs is the same as the inputs of contributing experts [55]. The GN output is the same as the number of the experts, here, ANN$_{FBC}$ and ANN$_{MPC}$. The MoE tries to compute a target from different paths (experts) to obtain the best possible performance of the global system. With a given set of training data $\{(x^\alpha, y^\alpha)\}$ where $y^\alpha = f^*(x^\alpha)$, a neural based network may solve the regression problem by learning a function $f$ that approximates $f^*$ by minimizing the following error function

$$E(W) = \frac{1}{2} \sum_\alpha \left( y^\alpha - f \left( x^\alpha, W \right) \right)^2 \qquad (20)$$

where $W$ is the weight matrix of gating network, $\alpha$ is the number of the training data. It has been proven that a maximum likelihood solution for weight matrix can be employed for Gaussian error ($f(x^\alpha, W) - y^\alpha$) [56], [57]. However, unrealistic to obtain a single function to model a wide range of data. To this reason, MoE technique employs a mixture of local experts by defining a gating network. As shown in Fig. 7, the output $u \sim y$ is computed through a weighted sum of experts' outputs. Thus

$$y = F(x, \theta) = \sum_{j=1}^{2} g_j(x, V) f_j(x, W_j) \qquad (21)$$

It should be mentioned that $\theta = (V, W_1, W_2)$ represents all the global model parameters. The condition of $g_1 + g_2 = 1$ leads to consider the $g_j$ as the softmax function of the output layer values $S_j$ of gating network. Thus

$$g_j(\boldsymbol{x}, \boldsymbol{V}) = \frac{e^{s_j(x,V)}}{\sum_k e^{s_k(x,V)}} \qquad (22)$$

Which may denotes a probability interpretation of the weights in $g_1$ and $g_2$. Rewrite equation (20) in terms of $\theta$, the solution of the problem is embedded in minimizing the following equation

$$E(\boldsymbol{\theta}) = \frac{1}{2} \sum_\alpha \left(y^\alpha - F\left(\boldsymbol{x}^\alpha, \boldsymbol{\theta}\right)\right)^2 \qquad (23)$$

Consider that a random process generates $\boldsymbol{x}$ from a given density functin and an expert is randomly chosen based on the gating probabiliy $g_j(\boldsymbol{x})$. Then the selected expert $j$ denotes a random variable with the mean of $u_j = f_j(\boldsymbol{x}, \boldsymbol{W}_j)$. Accordingly, the switching function $u \sim y$ is the expected value of $E(y_j|\boldsymbol{x})$. Thus one can obtain the probability of $(\boldsymbol{x},y)$ as

$$
\begin{aligned}
P(\boldsymbol{x}, y|\boldsymbol{\theta}) &= \sum_j g_j(\boldsymbol{x}, \boldsymbol{V}) P(j, \boldsymbol{x}, y|\boldsymbol{W}) \\
&= \sum_j g_j(\boldsymbol{x}, \boldsymbol{V}) \mathscr{N}_j e^{-\frac{1}{2\sigma_j^2}(y-f(x,W_j))^2} \qquad (24)
\end{aligned}
$$

where $N_j$ is a normalization factor. If the pair set of $\{(\boldsymbol{x}^\alpha, y^\alpha)\}$ is assumed to be independence, log-likelihood can be applied as follows:

$$
\begin{aligned}
L(\boldsymbol{\theta}) &= \prod_\alpha P(\boldsymbol{x}^\alpha, y^\alpha|\boldsymbol{\theta}) \\
&= \sum_\alpha log \sum_j g_j(\boldsymbol{x}^\alpha, \boldsymbol{V}) \mathscr{N}_j e^{-\frac{1}{2\sigma_j^2}(y^\alpha - f(\boldsymbol{x}^\alpha, W_j))^2} \qquad (25)
\end{aligned}
$$

Using expectation maximisation [58], one can find the optimal set of $\boldsymbol{\theta}^*$ parameters. It was proven that the gradient descent of log-likelihood $(-\nabla_{\boldsymbol{\theta}} L)$ converges faster and more reliable in comparison with $E(\boldsymbol{\theta})$. Accordingly, by calculating and extracting the optimum parameters in $\boldsymbol{\theta}$ from equation (24), the MoE based controlling strategy which is instructed from two powerful controlling strategies i.e. MPC and FBC becomes ready to be implemented in the real environment.

## V. RESULTS AND DISCUSSION
### A. EXPERIMENTAL RESULTS
In this section, our proposed controlling strategy i.e. mixture of experts has been designed and implemented in the STM32f407VGT6 microcontroller for controlling a DC-DC boost converter (Fig. 2) in the electric vehicles. The DC-DC BPEC is assumed to supply the required energy from a 200V input to a 400V output for an electric motor drive. Full rated power of the considered DC-DC BPEC is 2000W. For a desired output voltage and input current ripples, a capacitor bank of $33\mu F$ and an inductor of 2mH were used in

the power circuit. Switching frequency was fixed at 10kHz. Fig. 8 demonstrates the performance of the DC-DC BPEC in three different controlling strategies. Fig. 8a illustrates the behavior of the DC-DC BPEC under a voltage reference variation in all three controlling strategies. The voltage reference has been changed from 360V to 400V. In all plots, orange and blue waveforms are allocated to the output capacitor voltage and input inductor current, respectively. As shown in this figure, all the strategies perfectly controlled the DC-DC BPEC in a stable condition with a desired steady-state error. Feedback controlling (FBC) strategy demonstrates the best conditions as the steady-state error and voltage and current ripples points of view. While model predictive controlling (MPC) demonstrates the best performance as the voltage under/overshoot and the settling time points of view. In Figs. 8a and 8b (the two most left plots), the minimum steady-state output voltage error occurred in the FBC controller in which the controlling signal continuously varied in order to stabilize the output capacitor voltage. The maximum steady-state error in the output voltage occurred in the case of MPC controlling strategy in which the behavior of the circuit is predicted through the inductor current and the capacitor voltage from their states in the previous switching period. Since, the prediction established based on the circuit parameters, the accuracy of the converter steady-state depends on how accurate the circuit parameters are inserted into the model. Current and voltage ripples were in their minimum values while FB controlling strategy was employed. Both capacitor voltage and inductor current ripples experienced higher values in the MP controlling strategy in the identical conditions. In addition to electromagnetic interference increase in the power converter, this increase in the ripples may also affect the useful lifetime of the power converter. Since the voltage and current stresses on the switches were minimized in the feedback controlling strategy, the total power loss of DC-DC BPEC is lower than that of in model predictive controlling strategy. On other side, dynamic performance of DC-DC BPEC with model predictive controlling strategy was by far better than that of using feedback controlling strategy. Maximum over/undershoot either in capacitor voltage and inductor current is allocated to the FBC strategy. In regard of the settling time, MPC strategy demonstrates better performance in comparison with FBC strategy. As illustrated, both FBC and MPC controlling strategies have their own merits due to their inherent controlling characteristics. The solution for exploiting both of their merits is to simultaneously employ both controlling strategies. Accordingly, as described, the proposed MoE controlling strategy has been used for DC-DC BPEC controlling. The performance of DC-DC BPEC has been enhanced using our proposed MoE controlling strategies. The rightmost plots in Figs. 8a and 8b are the corresponded waveforms while MoE controlling strategy was applied to the DC-DC BPEC. As previously mentioned, both FBC and MPC as the experts have their own share on the controlling parameters ($u$) by training the networks shown in Fig. 7. Both $ANN_{FBC}$ and $ANN_{MPC}$
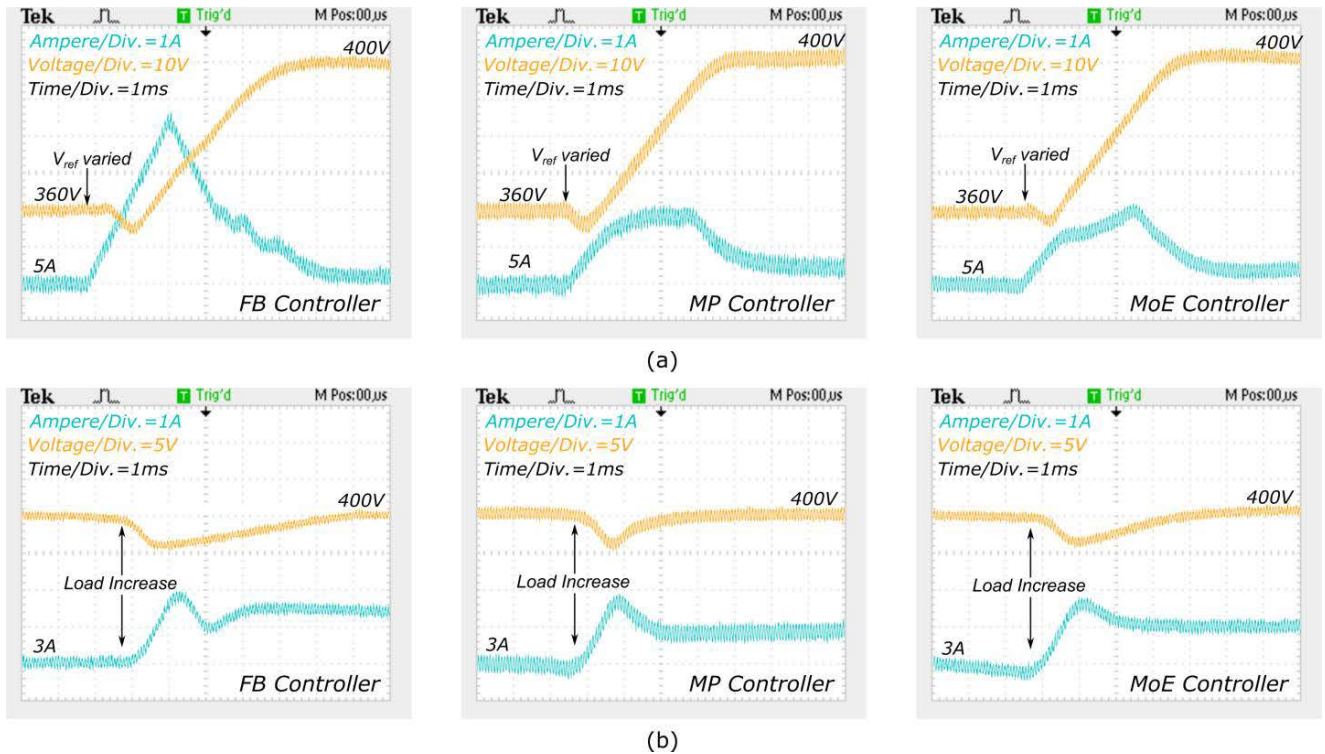
**FIGURE 8.** Experimental results of inductor current and capacitor voltage with different controlling strategies under different conditions. a) DC-DC BPEC performance under voltage reference variation in which voltage reference has been changed from 360V to 400Vand b) DC-DC BPEC performance under a step change in the load.

have three hidden layers with the number of neurons of 40, 35, and 25, respectively. The gating network has two hidden layers with the number of neurons of 5 and 3, respectively. It is noteworthy that the number of hidden layers and their corresponded neurons were chosen as a trade of between the computational time and the accuracy with trial and errors. The gating network is responsible for deciding how much contribution is required for final controlling parameter i.e. $u(t)$ for each expert in order to optimize DC-DC BPEC performance under different conditions. These three ANNs were trained via distinct *1800* data from the real mission profile as described in the section III.A. Output capacitor voltage ($v_o$) and input inductor current ($i_L$) were chosen as the input of the neural networks and switching function ($u$) is considered as the ANN output for controlling the DC-DC BPEC. The gating ANN determines the share of each expert on the controlling parameters while minimizing the errors as described in eq. (24). The ANNs were computed offline and their weights were applied to microcontroller as the constants value to compute $u$ as the switching function. In fact, MoE strategy is a general mapping function in which the inputs ($v_o$ and $i_L$) are employed for extracting the output ($u$) via three ANNs.

Fig. 9 illustrates the contributions of the FBC and MPC strategies in the controlling of the considered DC-DC BPEC versus the input data i.e. input inductor current and output capacitor voltage. The plot demonstrates that the FBC
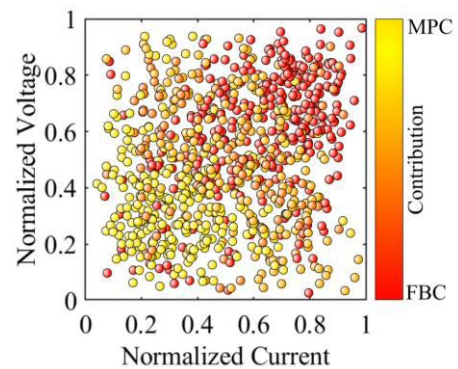


**FIGURE 9.** Model predictive and feedback strategies' contributions on controlling a DC-DC boost power electronic converter in the different operating points (WLTC-class3 mission profile). The voltage and current are normalized to their maximum tolerable values.

strategy generally has more contribution in the switching function i.e. $u(t)$ than MPC controller in the high input current and high output voltage as the input of expert in these controllers. Main contribution of MPC strategy in the controlling of the considered DC-DC BPEC is occurred in low current and low voltage operating points. In other operating points, both MPC and FBC approximately share the same contribution in controlling of the converter as also revealed from orange scatters in Fig. 9. In the high power operating

**TABLE 1.** Features of different controlling strategies in DC-DC BPEC.

| No | Controlling indices | FBC Proposed in [4] | MPC Proposed in [34] | ADLBC* Proposed in [35] | BAFBC** Proposed in [39] | DRLBC*** Proposed in [38] | MoE Proposed here |
|---|---|---|---|---|---|---|---|
| 1 | **Maximum Steady-state Error** | 0.5% | 2.2% | 0.8% | 0.4% | 1.2% | 0.8% |
| 2 | **Maximum Ripple** | 2.9% | 4.1% | 2.8% | 2.7% | 4.8% | 3.3% |
| 3 | **Maximum Over/undershoot** | 3.3% | 2.8% | 3.1% | 3.9% | 2.1% | 2.9% |
| 4 | **Maximum settling time** | 15ms | 2ms | 4ms | 14ms | 6ms | 2.7ms |
| 5 | **Full load efficiency** | 98.2% | 97.9% | 98.0% | 97.8% | 97.5% | 98.7% |
| 6 | **Implementation level** | Simple | simple | Complicated | Moderate | Complicated | Moderate |

\* adaptive deep learning-based controller
\*\* bat optimization algorithm for feedback controller
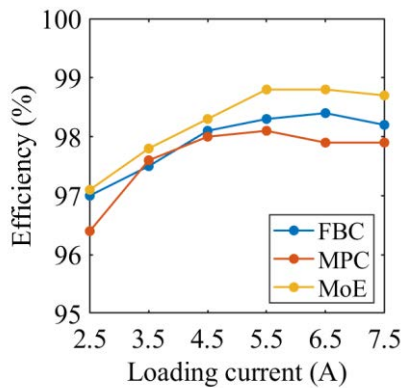\*\*\* deep reinforcement learning based controlling



**FIGURE 10.** Experimental efficiency measurements for Feedback, model predictive and mixture of expert controlling strategies versus loading current drawn from the considered DC-DC BPEC.

points, the parameter deviations of the key components in the circuit have become intensified. Although the observer in the MPC is in charge of minimizing this deviation in the control algorithm, the it may not thoroughly estimate the level of parameter deviation which finally leads to more error in dynamic and steady-state in high power operating points. Accordingly, FBC has better performance in the higher operating points. However, in the low operating points, MPC demonstrate a better performance in comparison with FBC due to its better dynamic behavior. The MoE strategy is trained in order to optimized the behavior of the converter in the different operating points. Thus, MPC dominates in lower operating points and FBC has higher contribution in converter controlling in higher operating points. Last but not least, the DC-DC BPEC efficiency is shown in Fig. 10. The efficiency of BPEC in all strategies improve by loading increase by 2%. Maximum efficiency was measured 98.6% in MoE strategy for BPEC controlling. It is also found that in all operating points MoE strategy has better performance as the efficiency point of view. The global behavior of the BPEC performance far improves while the proposed controlling strategy i.e. mixture of experts has been used. The reason is that the merits of both feedback and model predictive controllers are unified in controlling DC-DC power converter, while their weaknesses are less contributed.

## B. CRITICAL ANALYSIS AND DISCUSSION

The performance and controlling indices of the proposed method are compared with the other recent controlling strategies in this section. Both transient and steady state indices are considered. Table 1 lists different features of the DC-DC BPEC performance with different controlling strategies. It is revealed that the FBC based strategies including conventional FBC and optimized FBC with bat algorithm far outweighs in the steady-state behavior while the MPC strategy has better performance as the dynamic point of view. Although, adaptive and deep reinforcement controllers show better performance in some indices, they are not globally optimized and have detriments in other indices. Using MoE, however, one can find that FBC's and MPC's merits are included in the DC-DC BPEC performance. These results are originated from the fact that both FBC and MPC strategies have contributions in controlling the DC-DC BPEC. In every specific operating point, their contributions are optimized by trained gating neural networks via several pre-calculated data. The maximum steady-state error of the DC-DC BPEC with MoE strategy is limited to 0.8% which demonstrate an enhancement of 1.4% in comparison with MPC strategy. It is the case of maximum ripple in which there exists an 0.8% improvement in MoE in comparison with MPC. In the case of dynamic response, the MoE strategy shows much better performance in comparison with other methods. In addition, except conventional FBC and MPC, the implementation of MoE controller is less complicated with comparison with other adaptive controllers [35], [38], [39]. Thanks to the combination of two different controllers, namely FBC and MPC, global optimization of the controlling indices either in steady or dynamic states is achieved. However, it is noteworthy that MoE design and training totally depends on the application in which the converter is used. In other words, the MoE is trained based on a specific mission profile. Thus, MoE controller can be designed for a specific converter with a specific mission profile.

## VI. CONCLUSION

In this paper, a new controlling strategy for the DC-DC boost power electronic converter has been proposed based on which the advantages of different classic controlling methods,

namely feedback and model predictive strategies have been simultaneously taken. The proposed mixture of expert algorithm uses both strategies in BPEC controlling by defining a contribution list for these two strategies in switching function as the controlling parameter of DC-DC power converter. The results reveal that not only does the proposed algorithm enhance the steady-state behavior of the DC-DC power converter, but also the dynamic behavior of the converter is also optimized. The results reported in this study indicated that 2.2% steady state error in MPC decreased to 0.8% in MoE algorithm. The settling time of the power converter under external disturbance decreased from 15ms in FPC to 2.7ms in MoE controller. Although this study used FBC and MPC as the fundamental controlling strategies for training the mixture of expert network, other controlling strategies depending on the application in which power converter is working may also be used as the basis of MoE algorithm. The proposed MoE algorithm is generic, valid, and applicable to any other power electronic converters with different fundamental controlling algorithms. Definition of a global mission profile for training the MoE controlling technique can propose a general MoE which is under study and would be reported in the near future.

## REFERENCES

[1] X. Wang, M. Wu, L. Ouyang, and Q. Tang, "The application of GA-PID control algorithm to DC–DC converter," in *Proc. 29th Chin. Control Conf.*, 2010, pp. 3492–3496.

[2] Y. Cao, V. Samavatian, K. Kaskani, and H. Eshraghi, "A novel nonisolated ultra-high-voltage-gain DC–DC converter with low voltage stress," *IEEE Trans. Ind. Electron.*, vol. 64, no. 4, pp. 2809–2819, Apr. 2017.

[3] V. Samavatian and A. Radan, "A high efficiency input/output magnetically coupled interleaved buck–boost converter with low internal oscillation for fuel-cell applications: CCM steady-state analysis," *IEEE Trans. Ind. Electron.*, vol. 62, no. 9, pp. 5560–5568, Sep. 2015, doi: 10.1109/TIE.2015.2408560.

[4] V. Samavatian and A. Radan, "A novel low-ripple interleaved buck–boost converter with high efficiency and low oscillation for fuel-cell applications," *Int. J. Electr. Power Energy Syst.*, vol. 63, pp. 446–454, Dec. 2014, doi: 10.1016/j.ijepes.2014.06.020.

[5] V. Samavatian, H. Iman-Eini, and Y. Avenas, "Reliability assessment of multistate degraded systems: An application to power electronic systems," *IEEE Trans. Power Electron.*, vol. 35, no. 4, pp. 4024–4032, Apr. 2020, doi: 10.1109/TPEL.2019.2933063.

[6] V. Samavatian, H. Iman-Eini, Y. Avenas, and M. Samavatian, "Effects of creep failure mechanisms on thermomechanical reliability of solder joints in power semiconductors," *IEEE Trans. Power Electron.*, vol. 35, no. 9, pp. 8956–8964, Sep. 2020.

[7] S. Kapat and P. T. Krein, "A tutorial and review discussion of modulation, control and tuning of high-performance DC-DC converters based on small-signal and large-signal approaches," *IEEE Open J. Power Electron.*, vol. 1, pp. 339–371, 2020, doi: 10.1109/OJPEL.2020.3018311.

[8] V. Samavatian, M. Fotuhi-Firuzabad, P. Dehghanian, and F. Blaabjerg, "Reliability modeling of multistate degraded power electronic converters with simultaneous exposure to dependent competing failure processes," *IEEE Access*, vol. 9, pp. 67096–67108, 2021, doi: 10.1109/ACCESS.2021.3075974.

[9] V. Samavatian, M. Fotuhi-Firuzabad, M. Samavatian, P. Dehghanian, and F. Blaabjerg, "Correlation-driven machine learning for accelerated reliability assessment of solder joints in electronics," *Sci. Rep.*, vol. 10, no. 1, p. 14821, Dec. 2020, doi: 10.1038/s41598-020-71926-7.

[10] A. Stupar, T. McRae, N. Vukadinović, A. Prodić, and J. A. Taylor, "Multi-objective optimization of multi-level DC–DC converters using geometric programming," *IEEE Trans. Power Electron.*, vol. 34, no. 12, pp. 11912–11939, Dec. 2019, doi: 10.1109/TPEL.2019.2908826.

[11] K. Hariharan, S. Kapat, and S. Mukhopadhyay, "Constant off-time digital current-mode controlled boost converters with enhanced stability boundary," *IEEE Trans. Power Electron.*, vol. 34, no. 10, pp. 10270–10281, Oct. 2019, doi: 10.1109/TPEL.2019.2893428.

[12] G. Zhou, S. Mao, S. Zhou, Y. Wang, and T. Yan, "Discrete-time modeling and symmetrical dynamics of $V^2$-controlled buck converters with trailing-edge and leading-edge modulations," *IEEE J. Emerg. Sel. Topics Power Electron.*, vol. 8, no. 4, pp. 3995–4008, Dec. 2020, doi: 10.1109/JESTPE.2019.2925688.

[13] P. Midya, P. T. Krein, and M. F. Greuel, "Sensorless current mode control—An observer-based technique for DC–DC converters," *IEEE Trans. Power Electron.*, vol. 16, no. 4, pp. 522–526, Jul. 2001, doi: 10.1109/63.931070.

[14] P. Song, C. Cui, and Y. Bai, "Robust output voltage regulation for DC–DC buck converters under load variations via sampled-data sensorless control," *IEEE Access*, vol. 6, pp. 10688–10698, 2018, doi: 10.1109/ACCESS.2018.2794458.

[15] W. Tang, F. C. Lee, R. B. Ridley, and I. Cohen, "Charge control: Modeling, analysis, and design," *IEEE Trans. Power Electron.*, vol. 8, no. 4, pp. 396–403, Oct. 1993, doi: 10.1109/63.261009.

[16] P. Midya and P. T. Krein, "Noise properties of pulse-width modulated power converters: Open-loop effects," *IEEE Trans. Power Electron.*, vol. 15, no. 6, pp. 1134–1143, Nov. 2000, doi: 10.1109/63.892828.

[17] M. Anun, M. Ordonez, I. G. Zurbriggen, and G. G. Oggier, "Circular switching surface technique: High-performance constant power load stabilization for electric vehicle systems," *IEEE Trans. Power Electron.*, vol. 30, no. 8, pp. 4560–4572, Aug. 2015, doi: 10.1109/TPEL.2014.2358259.

[18] R. Redl and J. Sun, "Ripple-based control of switching regulators— An overview," *IEEE Trans. Power Electron.*, vol. 24, no. 12, pp. 2669–2680, Dec. 2009, doi: 10.1109/TPEL.2009.2032657.

[19] T. Qian, "Subharmonic analysis for buck converters with constant on-time control and ramp compensation," *IEEE Trans. Ind. Electron.*, vol. 60, no. 5, pp. 1780–1786, May 2012, doi: 10.1109/TIE.2012.2190375.

[20] J. Chen, A. Prodic, R. W. Erickson, and D. Maksimovic, "Predictive digital current programmed control," *IEEE Trans. Power Electron.*, vol. 18, no. 1, pp. 411–419, Jan. 2003, doi: 10.1109/TPEL.2002.807140.

[21] A. Ugur and M. Yilmaz, "Digital hybrid current mode control for DC–DC converters," *IET Power Electron.*, vol. 12, no. 4, pp. 891–898, 2019.

[22] E. Abdelhamid, L. Corradini, P. Mattavelli, G. Bonanno, and M. Agostinelli, "Sensorless stabilization technique for peak current mode controlled three-level flying-capacitor converters," *IEEE Trans. Power Electron.*, vol. 35, no. 3, pp. 3208–3220, Mar. 2020, doi: 10.1109/TPEL.2019.2930011.

[23] H. Kumar, R. Channappanavar, and S. K. Mishra, "High bandwidth inductor current estimator for digitally controlled DC–DC converters for light load applications," *IEEE J. Emerg. Sel. Topics Power Electron.*, vol. 9, no. 6, pp. 6681–6691, Dec. 2021, doi: 10.1109/JESTPE.2021.3105598.

[24] G. Zhou, G. Mao, H. Zhao, S. Zhou, and P. Mattavelli, "Digital average-ripple-based control techniques for switching converters with fast transient performance," *IEEE J. Emerg. Sel. Topics Power Electron.*, vol. 9, no. 1, pp. 89–101, Feb. 2021, doi: 10.1109/JESTPE.2020.2964268.

[25] V. Samavatian, F. Mardani, and M. Nourmohammadpour, "A novel low current ripple magnetically coupled interleaved DC–DC buck-boost converter with high efficiency and continuous transfer-function for fuel-cell applications," *Int. J. Sci. Eng. Res.*, vol. 6, no. 3, 2015. [Online]. Available: http://www.ijser.org

[26] P. Peltoniemi, P. Nuutinen, and J. Pyrhonen, "Observer-based output voltage control for DC power distribution purposes," *IEEE Trans. Power Electron.*, vol. 28, no. 4, pp. 1914–1926, Apr. 2013, doi: 10.1109/TPEL.2012.2213273.

[27] G. Joos, P. D. Ziogas, and D. Vincenti, "A model reference adaptive PWM technique," *IEEE Trans. Power Electron.*, vol. 5, no. 4, pp. 485–494, Oct. 1990, doi: 10.1109/63.60693.

[28] L. Cheng, P. Acuna, R. P. Aguilera, M. Ciobotaru, and J. Jiang, "Model predictive control for DC–DC boost converters with constant switching frequency," in *Proc. IEEE 2nd Annu. Southern Power Electron. Conf. (SPEC)*, Dec. 2016, pp. 1–6, doi: 10.1109/SPEC.2016.7846189.

[29] P. Karamanakos, T. Geyer, and S. Manias, "Direct voltage control of DC-DC boost converters using enumeration-based model predictive control," *IEEE Trans. Power Electron.*, vol. 29, no. 2, pp. 968–978, Feb. 2014, doi: 10.1109/TPEL.2013.2256370.

[30] H. Chen, S. Tang, D. Wang, C. Zhang, Z. Zeng, and J. Wang, "Model predictive control based on state-space averaging model for three-level flying capacitor boost converter with constant switching frequency and improved dynamic performance," in *Proc. IEEE 9th Int. Power Electron. Motion Control Conf. (IPEMC-ECCE Asia)*, Nov. 2020, pp. 3051–3056, doi: 10.1109/IPEMC-ECCEAsia48364.2020.9368202.

[31] V. Prabhu and P. Damodharan, "Explicit model predictive control of quadratic boost converter for high step-up applications," in *Proc. IEEE Int. Conf. Power Electron., Drives Energy Syst. (PEDES)*, Dec. 2018, pp. 1–5, doi: 10.1109/PEDES.2018.8707638.

[32] M. Hejri and H. Mokhtari, "Hybrid modeling and control of a DC–DC boost converter via extended mixed logical dynamical systems (EMLDs)," in *Proc. 5th Annu. Int. Power Electron., Drive Syst. Technol. Conf. (PED-STC)*, Feb. 2014, pp. 373–378, doi: 10.1109/PEDSTC.2014.6799403.

[33] H.-P. Ren, M.-M. Zheng, and J. Li, "A simplified mixed logical dynamic model and model predictive control of boost converter with current reference compensator," in *Proc. IEEE 24th Int. Symp. Ind. Electron. (ISIE)*, Jun. 2015, pp. 61–65, doi: 10.1109/ISIE.2015.7281444.

[34] L. Cheng, P. Acuna, R. P. Aguilera, J. Jiang, S. Wei, J. E. Fletcher, and D. D. C. Lu, "Model predictive control for DC–DC boost converters with reduced-prediction horizon and constant switching frequency," *IEEE Trans. Power Electron.*, vol. 33, no. 10, pp. 9064–9075, Oct. 2018, doi: 10.1109/TPEL.2017.2785255.

[35] K. Yu, F. Zhuo, F. Wang, T. Zhu, and Y. Gou, "Adaptive deep-learning-based steady-state modeling and fast control strategy for CLLC DC–DC converter in highly renewable penetrated system," *IEEE J. Emerg. Sel. Topics Circuits Syst.*, vol. 12, no. 1, pp. 205–219, Mar. 2022, doi: 10.1109/JETCAS.2022.3152063.

[36] C. Cui, N. Yan, B. Huangfu, T. Yang, and C. Zhang, "Voltage regulation of DC–DC buck converters feeding CPLs via deep reinforcement learning," *IEEE Trans. Circuits Syst. II, Exp. Briefs*, vol. 69, no. 3, pp. 1777–1781, Mar. 2022, doi: 10.1109/TCSII.2021.3107535.

[37] Y. Tang, W. Hu, J. Xiao, Z. Chen, Q. Huang, Z. Chen, and F. Blaabjerg, "Reinforcement learning based efficiency optimization scheme for the DAB DC–DC converter with triple-phase-shift modulation," *IEEE Trans. Ind. Electron.*, vol. 68, no. 8, pp. 7350–7361, Aug. 2021, doi: 10.1109/TIE.2020.3007113.

[38] M. Gheisarnejad, H. Farsizadeh, and M. H. Khooban, "A novel nonlinear deep reinforcement learning controller for DC–DC power buck converters," *IEEE Trans. Ind. Electron.*, vol. 68, no. 8, pp. 6849–6858, Aug. 2021, doi: 10.1109/TIE.2020.3005071.

[39] S.-Y. Chen, B.-C. Yang, T.-A. Pu, C.-H. Chang, and R.-C. Lin, "Active current sharing of a parallel DC–DC converters system using bat algorithm optimized two-DOF PID control," *IEEE Access*, vol. 7, pp. 84757–84769, 2019, doi: 10.1109/ACCESS.2019.2925064.

[40] A. F. Minai, T. Usmani, A. Iqbal, and M. A. Mallick, "Artificial bee colony based solar PV system with Z-source multilevel inverter," in *Proc. Int. Conf. Adv. Comput., Commun. Mater. (ICACCM)*, Aug. 2020, pp. 187–193, doi: 10.1109/ICACCM50413.2020.9213060.

[41] M. N. Uddin, M. A. Abido, and M. A. Rahman, "Real-time performance evaluation of a genetic-algorithm-based fuzzy logic controller for IPM motor drives," *IEEE Trans. Ind. Appl.*, vol. 41, no. 1, pp. 246–252, Jan. 2005, doi: 10.1109/TIA.2004.840995.

[42] A. Divakar and J. Jacob, "Genetic algorithm based tuning of nonfragile and robust PI controller for PSFB DC–DC converter," in *Proc. Int. Conf. Commun. Electron. Syst. (ICCES)*, Jul. 2019, pp. 1846–1851, doi: 10.1109/ICCES45898.2019.9002210.

[43] V. Samavatian and A. Radan, "A high efficiency Input/Output magnetically coupled interleaved buck–boost converter with low internal oscillation for fuel-cell applications: CCM steady-state analysis," *IEEE Trans. Ind. Electron.*, vol. 62, no. 9, pp. 5560–5568, Sep. 2015, doi: 10.1109/TIE.2015.2408560.

[44] Y. Yang, H. Wang, F. Blaabjerg, and T. Kerekes, "A hybrid power control concept for PV inverters with reduced thermal loading," *IEEE Trans. Power Electron.*, vol. 29, no. 12, pp. 6271–6275, Dec. 2014, doi: 10.1109/TPEL.2014.2332754.

[45] C. Wang, J. Li, Y. Yang, and F. Ye, "Combining solar energy harvesting with wireless charging for hybrid wireless sensor networks," *IEEE Trans. Mobile Comput.*, vol. 17, no. 3, pp. 560–576, Mar. 2018, doi: 10.1109/TMC.2017.2732979.

[46] V. Samavatian, "A systematic approach to reliability assessment of DC–DC power electronic converters," Univ. Tehran, Universite Grenoble Alpes, Tehran, Iran, Tech. Rep. 2019GREAT028, 2019.

[47] W. Ming and J. Liu, "A new experimental study of input-output feedback linearization based control of boost type DC/DC converter," in *Proc. IEEE Int. Conf. Ind. Technol.*, Jul. 2010, pp. 685–689, doi: 10.1109/ICIT.2010.5472720.

[48] F. P. Priya and K. Latha, "Feedback linearization control of boost converter," in *Proc. 2nd Int. Conf. Intell. Comput., Instrum. Control Technol. (ICICICT)*, Jul. 2019, pp. 169–173, doi: 10.1109/ICICICT46008.2019.8993341.

[49] S. Wang, T. Dragicevic, G. F. Gontijo, S. K. Chaudhary, and R. Teodorescu, "Machine learning emulation of model predictive control for modular multilevel converters," *IEEE Trans. Ind. Electron.*, vol. 68, no. 11, pp. 11628–11634, Nov. 2021, doi: 10.1109/TIE.2020.3038064.

[50] T. Dragičević, P. Wheeler, and F. Blaabjerg, "Artificial intelligence aided automated design for reliability of power electronic systems," *IEEE Trans. Power Electron.*, vol. 34, no. 8, pp. 7161–7171, Aug. 2019, doi: 10.1109/TPEL.2018.2883947.

[51] S. Wen, Y. Wang, Y. Tang, Y. Xu, P. Li, and T. Zhao, "Real-time identification of power fluctuations based on LSTM recurrent neural network: A case study on Singapore power system," *IEEE Trans. Ind. Informat.*, vol. 15, no. 9, pp. 5266–5275, Sep. 2019, doi: 10.1109/TII.2019.2910416.

[52] V. Samavatian, M. Fotuhi-Firuzabad, M. Samavatian, P. Dehghanian, and F. Blaabjerg, "Iterative machine learning-aided framework bridges between fatigue and creep damages in solder interconnections," *IEEE Trans. Compon., Package., Manuf. Technol.*, vol. 12, no. 2, pp. 349–358, Feb. 2022, doi: 10.1109/TCPMT.2021.3136751.

[53] R. Calvin and S. Suresh, "Image captioning using convolutional neural networks and recurrent neural network," in *Proc. 6th Int. Conf. Converg. Technol. (ICT)*, Apr. 2021, pp. 1–4, doi: 10.1109/I2CT51068.2021.9418001.

[54] Y. Chu, J. Fei, and S. Hou, "Adaptive global sliding-mode control for dynamic systems using double hidden layer recurrent neural network structure," *IEEE Trans. Neural Netw. Learn. Syst.*, vol. 31, no. 4, pp. 1297–1309, Apr. 2020, doi: 10.1109/TNNLS.2019.2919676.

[55] S. E. Yuksel, J. N. Wilson, and P. D. Gader, "Twenty years of mixture of experts," *IEEE Trans. Neural Netw. Learn. Syst.*, vol. 23, no. 8, pp. 1177–1193, Aug. 2012.

[56] C. Bauckhage and C. Thurau, "Exploiting the fascination: Video games in machine learning research and education," in *Proc. 2nd Int. Workshop Comput. Game Design Technol.*, 2004, pp. 61–70.

[57] B. Tang, M. I. Heywood, and M. Shepherd, "Input partitioning to mixture of experts," in *Proc. Int. Joint Conf. Neural Netw. (IJCNN)*, 2002, vol. 1, pp. 227–232.

[58] A. P. Dempster, N. M. Laird, and D. B. Rubin, "Maximum likelihood from incomplete data via the EM algorithm," *J. Roy. Stat. Soc. B, Methodol.*, vol. 39, no. 1, pp. 1–22, 1977.

**MOHSEN MOHAMMADZADEH** received the B.Sc. and M.Sc. degrees in power engineering from the Babol Noshirvani University of Technology, Babol, Iran, in 2014 and 2022, respectively.

His research interests include converters, renewable energy, electric vehicles. Moreover, he posseses over seven years of experience as a supervisor and a designer in several engineer companies.

**EHSAN AKBARI** was born in Borujerd, Iran, in 1987. He received the B.Sc. and M.Sc. degrees in power electrical engineering from the Mazandaran University of Science and Technology (MUST), Babol, Iran, in 2010 and 2014, respectively. He has published more than 125 papers in reputed journals and conferences. His research interests include power quality and distribution flexible AC transmission systems (DFACTS), application of power electronics in power systems, power electronics multilevel converters, smart grids, harmonics and reactive power control using hybrid filters, and renewable energy systems. He is a contributing Reviewer of *AJEEE* journal.

**ANAS A. SALAMEH** has been an Associate Professor with the Department of Management Information Systems, College of Business Administration, Prince Sattam Bin Abdulaziz University, since 2016. He is currently the Deputy Director of the students' activities committee as well as a member of the exams scheduling committee, PSAU. His major research interests include the area such as e-commerce (m-commerce), e-business, e-marketing, technology acceptance/adoption, e-learning, e-CRM, and service quality. He evaluated service quality in many areas related to e-services aspects.

**SASAN PIROUZI** received the B.Sc. degree in electrical engineering from the Technical and Vocational University, Mashhad, Iran, in 2012, the M.Sc. degree from the Isfahan University of Technology, Isfahan, Iran, in 2014, and the Ph.D. degree from the Shiraz University of Technology (SUTECH), Shiraz, Iran, in 2017. His research interests include power system operation and planning, electric vehicles, DERs, and the application of optimization methods in power systems.

**MOJTABA GHADAMYARI** (Member, IEEE) received the degree in electrical engineering from Shahid Beheshti University, Tehran, Iran. He has been written and co-operated more than five articles in some fields such as reliability, distributed generation, energy, renewable resource microgrid, and renewable energy. His current research interest includes power systems.

**TOMONOBU SENJYU** (Senior Member, IEEE) received the B.S. and M.S. degrees in electrical engineering from the University of the Ryukyus, in 1986 and 1988, respectively, and the Ph.D. degree in electrical engineering from Nagoya University, in 1994. Since 1988, he has been with the Department of Electrical and Electronics Engineering, Faculty of Engineering, University of the Ryukyus, where he is currently a Professor. His research interests include the areas of power system optimization and operation, advanced control, renewable energy, the IoT for energy management, ZEH/ZEB, smart city, and power electronics. He is a member of the Institute of Electrical Engineers of Japan.

• • •